SUPPORTING INFORMATION

for

New insights into the coordination chemistry and molecular structure

of copper(II) histidine complexes in aqueous solutions
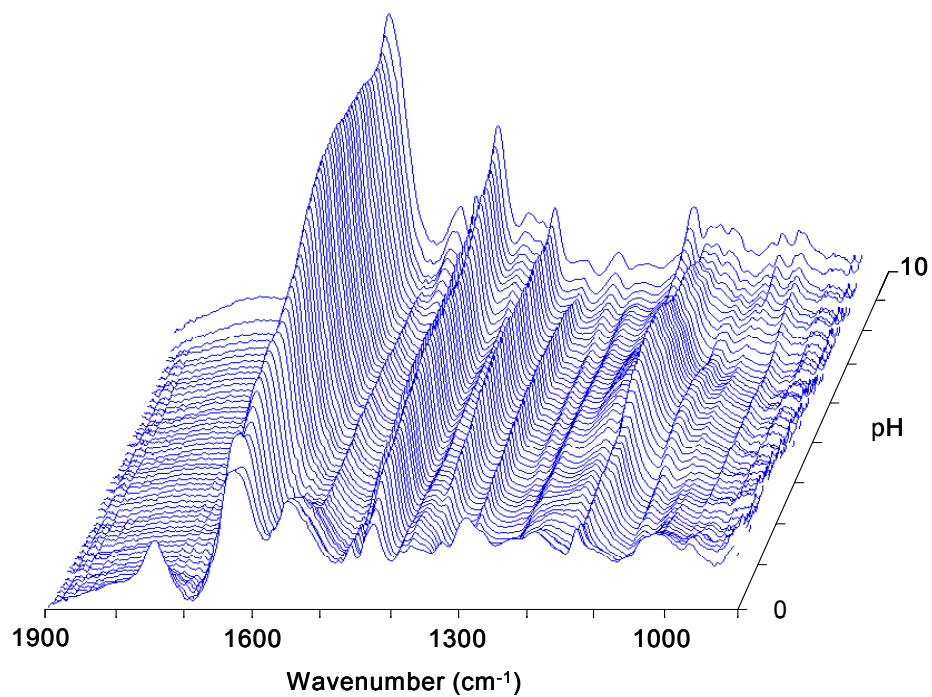
J. Gerbrand Mesu[1], Tom Visser[1], Fouad Soulimani[1], Ernst E. van Faassen[2],

Peter de Peinder[3], Andrew M. Beale[1] and Bert M. Weckhuysen[1*]

Debye Institute, [1]Department of Inorganic Chemistry and Catalysis, [2]Interface Physics,

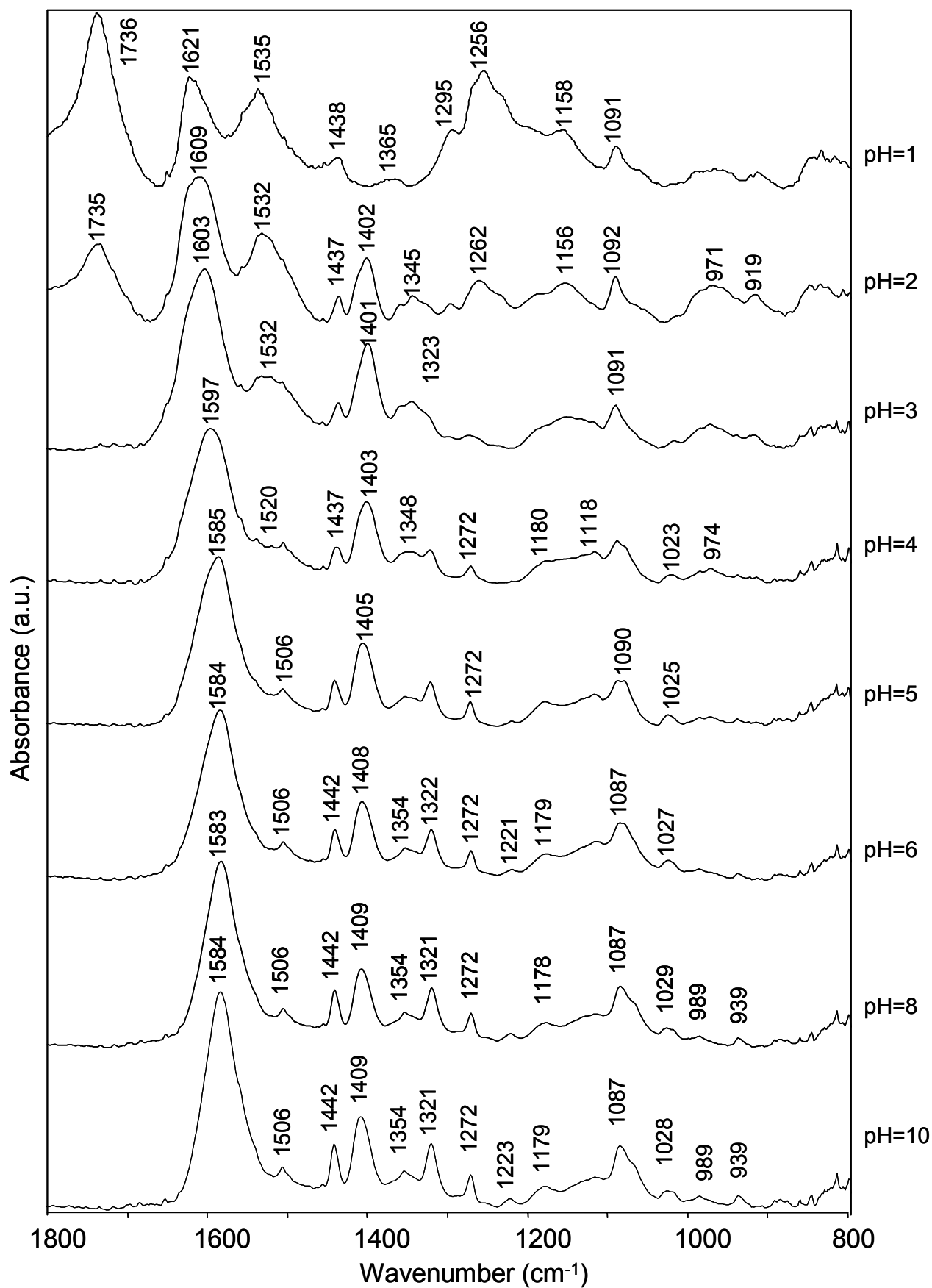Utrecht University, Sorbonnelaan 16, 3584 CA Utrecht, The Netherlands

[3]Vibspec, Haaftenlaan 28, 4006 XL Tiel, The Netherlands

* To whom correspondence should be send. E-mail: b.m.weckhuysen@chem.uu.nl
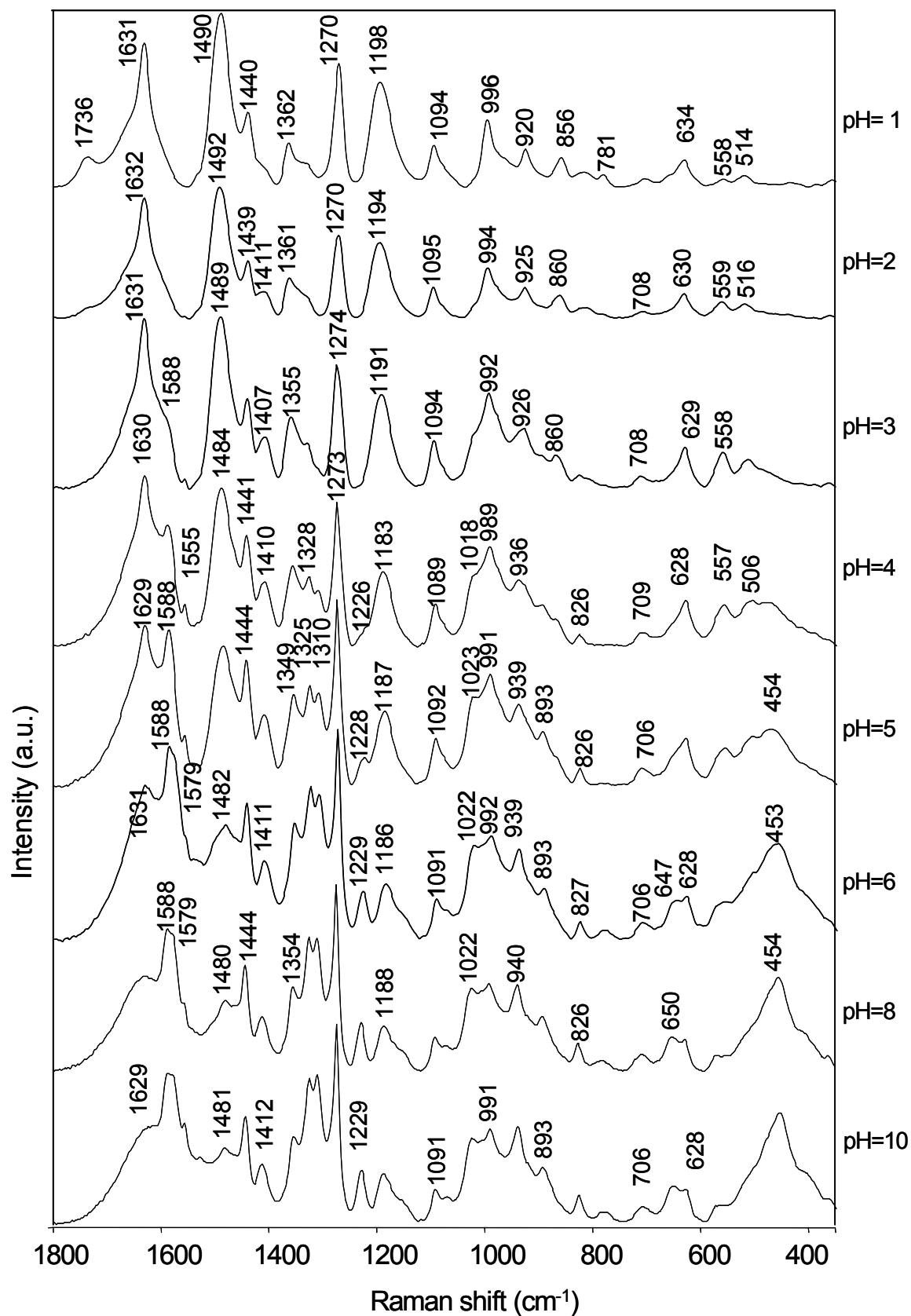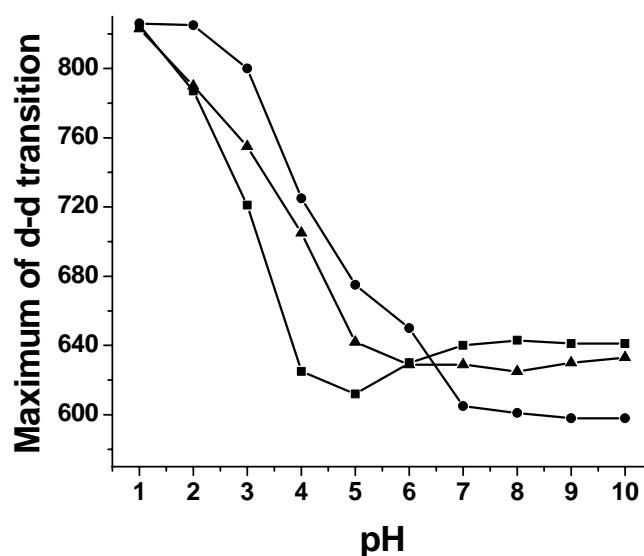
Figure S1. 3D plot of IR spectra of Cu^{2+}/His recorded during the titration experiment from pH = 0.3 to 10.

Figure S2. IR spectra of Cu^{2+}/His solutions at pH = 1 (top) to pH = 10 (bottom).
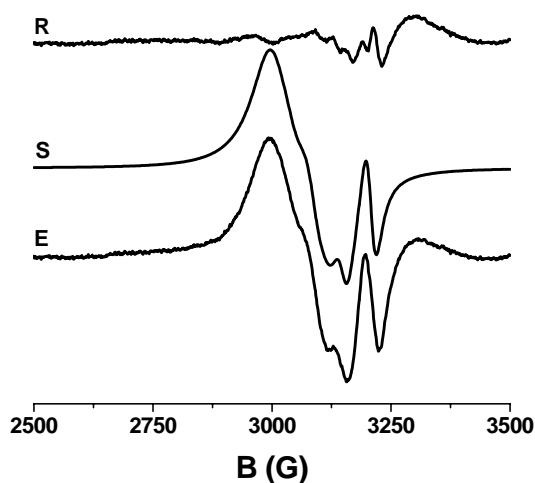
Figure S3. Raman spectra of Cu^{2+}/His solutions at pH = 1 (top) to pH = 10 (bottom).

Figure S4. The maximum of the copper d-d transition as function of the solution pH for aqueous solutions
of Cu^{2+}/His (-■-), $Cu^{2+}/$ glycine (-▲-) and $Cu^{2+}/$ histamine(-●-).

ESR analysis

To illustrate the results of the calculations, the simulated spectrum of the $Cu^{2+}/$**his** solution at pH = 2.0 is presented in figure S5, together with the experimental spectrum and the residual that remains after subtraction of the simulation from the experimental data. It is shown that the main contribution (about 85%) at pH = 2 originates from a complex with a relatively high g_0 and low A_0 value. Furthermore, the spectrum of a second species (estimated 15%) with a much lower g_0- and higher A_0 value is present, superimposed on the spectrum of the main complex. Finally, the residual spectrum points to a minor contribution of a third copper species. A similar simulation and interpretation process has been followed for the spectra obtained at the other pH-values.


Figure S5. The experimental ESR spectrum (E), the result of the simulation (S) and the residual (R) of the $Cu^{2+}/$His solution at pH = 2.0.

S4

XAFS analysis

The X-ray absorption near edge structures (XANES) of the X-ray absorption spectra of four Cu^{2+}/**his** samples, the background subtracted EXAFS data (k^1 weighted) at various pHs and the associated Fourier Transforms (including both the real part and the transform envelope) are presented in Figures S6-S8, respectively. The differences between the spectra are very small, but closer examination revealed a small but significant shift for the start of the oscillations towards a lower k-space value with increasing pH. It is unlikely that this shift is due to a change in the oxidation state of copper since the position of the Cu K-edge did not change. However, it is well known that such a shift, which is also associated with an increase in the EXAFS oscillation frequency, is related to an increase in the average absorber-scatterer distance.[61] Since the shift is observed at low k-space values, it implies that it corresponds to changes in the first Cu^{2+}/His coordination shell. The corresponding Fourier Transforms confirm these observations, as the centroid position of the peaks from the real part of the transform is shifted towards higher r-values. From a comparison of these positions, it can be concluded that the bond distance sequence as a function of the pH is: pH = 2.0 $\approx$ pH = 2.9 $\approx$ pH = 3.4 < pH = 4.4 < pH = 6.0 < pH = 7.3 $\approx$ pH = 8.0.

Fitting of the EXAFS data was also performed and the results are shown in Table S1. Most notably, the best fit for the first shell for the samples pH = 2.0, 2.9 and 3.4 is obtained with 4 oxygen atoms at a distance of 1.95 Å. At pH = 4.4 this distance has increased to 1.96 Å, although a tendency towards under-coordination (CN < 4.0) was observed. This finding probably reflects a gradual increase in the number of nitrogen atoms present in the first coordination sphere and indeed for pH = 6.0, 7.3 and 8.0 better R-values were obtained when considering 4 nitrogen atoms as nearest neighbours at a distance of 1.98 – 1.99 Å. Whilst we note that the error in the determination of bond distances by fitting the EXAFS is *ca* 0.02 Å (1%),[62] it is clear that the parameters derived by this process closely follow the variation observed in r- and k-space. Therefore, it is concluded that the refined differences of 0.01 Å observed between pH = 3.4, 4.4, 6.0 and 7.3 are real. Finally, it should be noted that the observed Debye-Waller factors are typical for these species in solution.[6]
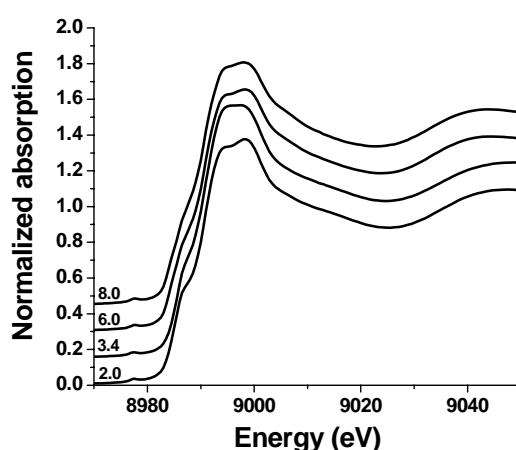
Figure S6. The XANES regions of the aqueous Cu^{2+}/His solution at different pH values (indicated in Figure).
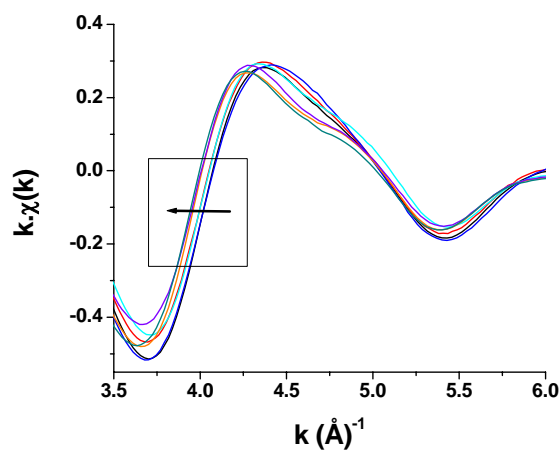
Figure S7. Phase-corrected k^1-weighted EXAFS spectra recorded at various pH's. Note that data are k^1-weighted in order to emphasise the changes that occur in the first shell of the Cu^{2+}/His complex.
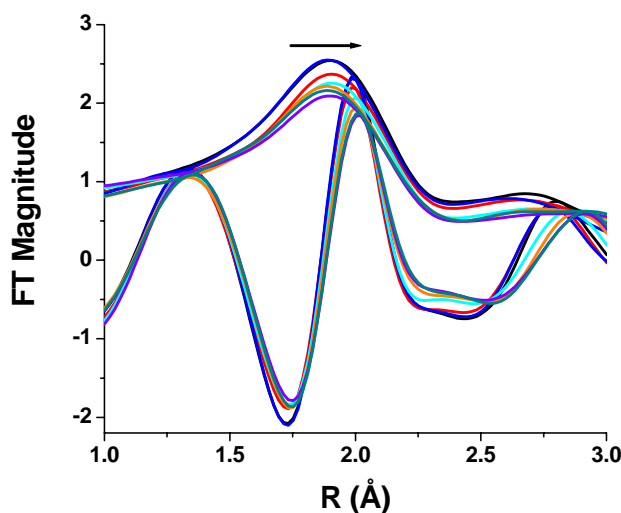
Figure S8. Associated Fourier Transforms for the data shown in Figure S6. Both the real part and the envelope are presented. The shift in the position of the centroid of the peaks in the real part indicates that the bond distance between copper and its nearest neighbours follows the trend pH = 2.0 ≈ pH = 2.9 ≈ pH = 3.4 < pH = 4.4 < pH = 6.0 < pH = 7.3 ≈ pH = 8.0.

Table S1. Parameters derived from a 1st shell analysis of k^1-weighted EXAFS data.

pH	r (Å)	CN	Ligand	$\sigma^2(\text{Å})^2$	E_f
2.0	1.95	4.3	O	0.015	0.59
2.9	1.96	3.9	O	0.013	0.00
3.4	1.95	4.4	O	0.014	0.93
4.4	1.96	3.7	O	0.013	-0.66
6.0	1.99	4.4	N	0.012	1.19
7.3	1.98	4.0	N	0.010	-0.08
8.0	1.99	4.4	N	0.015	1.27

r(Å) = average 1st shell distance, CN = coordination number, E_f = Fermi energy, $\sigma^2(\text{Å})^2$ = Debye-Waller factor.

Multivariate curve resolution

Multivariate curve resolution (MCR) was carried out on 42 IR spectra, using model calculations in MatLab®. It was assumed that the solution with pH < 1.75 only contained $Cu(H_2O)_6$, while at pH > 10.07 only complex *h* was present. In these model calculations the spectra were fitted using 6 pure component spectra. The spectra of the solution at pH 1.75 and 10.07 were used as input for the pure component spectra of $Cu(H_2O)_6$ and complex *h* respectively. With the obtained knowledge from the ESR measurements the concentration of the six different species was forced to zero outside the pH regions shown in Table S2.

Table S2. pH regions where the contribution of the complexes is non-zero

|	pH region
$Cu(H_2O)_6$	1.75<pH<2.75
Complex c	1.75<pH<3.56
Complex e	2.55<pH<4.55
Complex f	3.15<pH<7.96
Complex g	4.75<pH<9.38
Complex h	5.15<pH<10.07

Non-negativity constraints were imposed on these calculations in order to obtain meaningful spectra and concentrations. The other four components and the scores of the different pure components (i.e. the concentrations of the different complexes) were obtained by solving equation 1. In this equation X is the data matrix, containing the 42 FT-IR ATR spectra of 374 data points in the area between 1050 and 1770 cm^{-1}. The concentration matrix C contains the 'concentrations' of the 6 pure components. The spectrum matrix S contains the pure component spectra, whereas E is the residual error matrix, which consists of the difference between the measured spectra and the spectra constructed from the linear combination of the pure component spectra.

$$X (42 \times 374) = C (42 \times 6) \bullet S (6 \times 374) + E (42 \times 374) \qquad (1)$$

A good fit was obtained, with a 99.35% fit of the total intensity in the infrared spectra. The six IR spectra corresponding to the 6 complexes are represented in Figure S9. The main contribution to the residual spectra originates from the water bending vibration around 1640 cm^{-1}. Addition of additional pure components to the model did not result in a better fit.

The component spectra of the complexes *c and e* and of the complexes *f, g* and *h* are virtually much the same. However, the resemblance between the component spectra *c* and *e* is understandable, as complex *c* is a mono-histidine complex, whereas complex *e* is a bis-histidine complex (in which the two histidine ligands are coordinating in the same way as the one histidine ligand in the mono-histidine complex). There are a few small differences between the component spectra of the complexes *f, g* and *h, but* major differences are not expected, as there is a lot of resemblance between the three complexes.
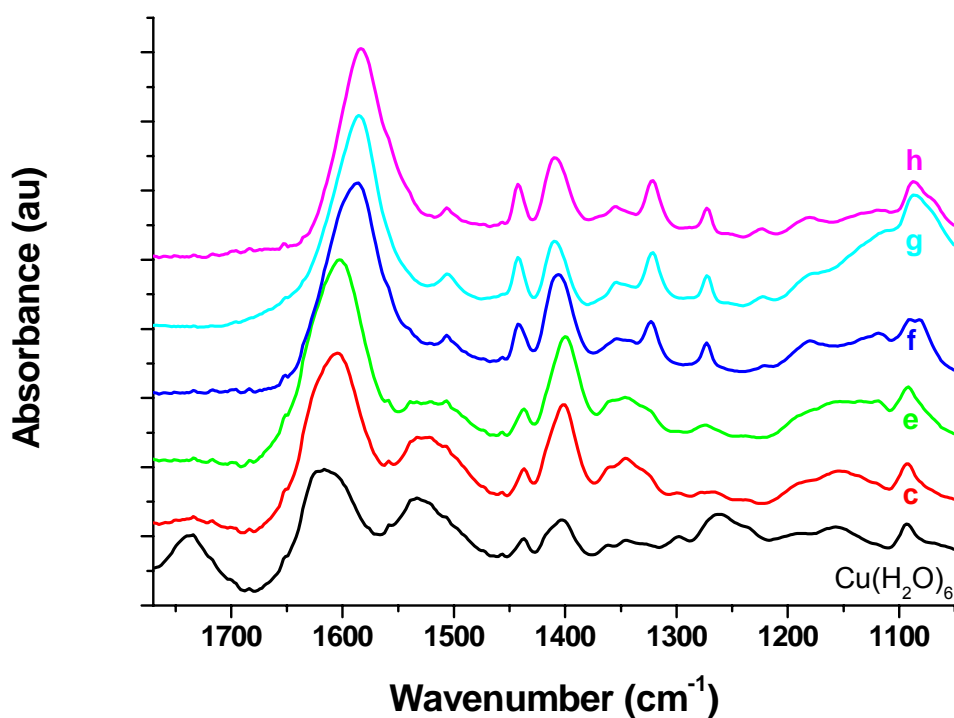
Figure S9. Component spectra of species after MCR analysis. The complexes are indicated in the graph.

Table S3. Observed infrared absorption frequencies and proposed assignments of aqueous CuHis solutions in the pH range 0-10.

pH=1	pH=2	pH=3	pH=4	pH=5	pH=6	pH=8	pH=10	Assignment
1736	1735							νC=O
1621	1620	1620						δ_{as} NH$_3^+$
	1609	1603	1597	1585	1584	1583	1584	ν_{as} CO$_2^-$
1535	1532	1532	1520					ν ring/δ_s NH$_3^+$
			1506	1506	1506	1506	1506	δN-H i.p./νC=N
1438	1437	1437	1437	1438	1442	1442	1442	δCH$_2$
	1402	1401	1403	1405	1408	1409	1409	ν_s CO$_2^-$
	1345	1346	1348	1348	1354	1354	1354	β NH$_3^+$
			1323	1322	1322	1322	1322	δCH$_2$ / δ =C-H
1295	1295							νC=N + δ =C-H
			1272	1272	1272	1272	1272	ν=C-N + δ C-H
1256	1262							ν_sC-O
			1180	1180	1179	1178	1179	
1091	1092	1091	1090	1090	1087	1087	1087	ν=C-N/δ=C-H(N$^\tau$)
			1023	1025	1027	1029	1028	νC-N side chain
991	991		990	991				ν=C-N / δ ring
	971	970	974					δ ring
920	919	919						δ =C-H i.p.

Table S4. Observed Raman shifts and proposed assignments of aqueous solutions of CuHis in the pH range 0-10.

pH=1	pH=2	pH=3	pH=4	pH=5	pH=6	pH=8	pH=10	Assignment
1736								ν C=O
1631	1632	1631	1630	1629	1631	1629	1629	ν C=C + ν C=N
	1588	1588	1588	1588	1588	1588	1588	ν C=C + ν C=N(N$^{\pi}$)
				1579	1579	1579	1579	ν C=C + δ N-H(N$^{\tau}$)
1490	1492	1489	1484	1484	1482	1480	1481	δ N-H i.p.
1440	1439	1440	1441	1444	1441	1444	1442	δ CH$_2$
	1411	1407	1410	1410	1411	1412	1412	δ CH-(CO$_2^-$)
1362	1361	1355	1355	1349	1350	1354	1354	δ CH$_2$/ν ring
		1328	1328	1325	1325	1325	1325	νC=N + ν C-N(N$^{\tau}$)
			1310	1310	1310	1310	1310	
1270	1270	1274	1273	1273	1274	1273	1270	δ =C-H (N$^{\pi}$)
1198	1194	1191	1183	1187	1186	1188	1188	ν N-C-N + δN-H i.p.
			1018	1023	1022	1022	1020	δ =C-H i.p. (N$^{\tau}$)
996	994	992	989	991	992	993	991	ν =C-N + δ ring (N$^{\pi}$)
920	925	926						=C-H i.p.
			936	939	939	940	940	=C-H i.p.
			893	893	893	893	893	
856	860	860	860					ν =C-C + δ ring
824	824	820	826	826	827	826	827	δ =C-H o.o.p.
634	630	629	628	628	628	627	628	δ ring
558	559	558	557	557				π CO$_2^-$
514	516	512	506					ν CO$_2^-$
			450	454	453	454	454	ν Cu-N